

# Infinite-Dimensional Feature Interaction

Chenhui Xu<sup>1,2</sup> Fuxun Yu<sup>1,3</sup> Maoliang Li<sup>4</sup> Zihao Zheng<sup>4</sup>

Zirui Xu<sup>1,5</sup> Jinjun Xiong<sup>2†</sup> Xiang Chen<sup>1,4†</sup>

<sup>1</sup> George Mason University <sup>2</sup>University at Buffalo

<sup>3</sup>Microsoft <sup>4</sup> Peking University <sup>5</sup>CVS Health

## Abstract

The past neural network design has largely focused on feature *representation space* dimension and its capacity scaling (e.g., width, depth), but overlooked the feature *interaction space* scaling. Recent advancements have shown shifted focus towards element-wise multiplication to facilitate higher-dimensional feature interaction space for better information transformation. Despite this progress, multiplications predominantly capture low-order interactions, thus remaining confined to a finite-dimensional interaction space. To transcend this limitation, classic kernel methods emerge as a promising solution to engage features in an infinite-dimensional space. We introduce InfiNet, a model architecture that enables feature interaction within an infinite-dimensional space created by RBF kernel. Our experiments reveal that InfiNet achieves new state-of-the-art, owing to its capability to leverage infinite-dimensional interactions, significantly enhancing model performance.

## 1 Introduction

In the past decade, deep neural network architecture design has experienced several major paradigm shifts regarding the feature representation learning. As shown in Fig. 1(a), the early stage of neural network design is dominant by flat stream architectures in the form of *weight-feature interaction* (e.g.,  $W\mathbf{x}$ ), like multi-layer perceptron (MLP), convolution neural networks (CNN), ResNet, etc. These models usually adopt linear superposition (e.g.,  $W_i\mathbf{x} \oplus W_j\mathbf{x}$ ) in the feature representation space. Therefore, the feature representation space scaling is limited to increase model channel width and depth [12, 16]. Nevertheless, this scaling approach has witnessed model development from the very small-scale MLPs or LeNet[17] to the recent huge ConvNext V2 [37]. With the ultra-scaled parameter amounts, computing complexity, and model size, the return of investment on model performance by further scaling feature dimensions has largely plateaued [9].

Despite the plateau in feature representation space, recent sporadic architecture design works [26] shed light on another potential dimension of scaling: feature interaction space. Specifically, as shown in Fig. 1(b), these neural network designs generally demonstrate *feature-feature interaction* (e.g.,  $W_i\mathbf{x} \otimes W_j\mathbf{x}$ ). As a mathematical example, the self-attention mechanism in Transformers [34] can be formulated as  $\mathbf{x}^{L+1} = f_k(\mathbf{x}^L) * f_q(\mathbf{x}^L) * f_v(\mathbf{x}^L)$ , which is also element-wise multiplication between processed input feature themselves. Characterized by element-wise interaction, these designs offer complementary feature correlation capabilities in addition to simple linear superposition. Such feature interactions have become the essential mechanisms of mainstream state-of-the-art neural architectures. For example, it's implemented in SENet with squeeze and excitation [15], non-local network with transposed multiplication [35], vision transformers with self-attention [3, 10, 34], gated aggregation [19, 31, 42], and quadratic neurons [11, 40, 41].

Although these models greatly improve the performance of state-of-the-arts, as mentioned above, these works provide diversified explanations that neglect the underlying shared design of element-wise feature multiplication operation [26], and thus may fail to reveal the fundamental source of improvement. To provide both explainability and quantifiability, in this paper, we propose a unified

† Corresponding Authors. Preprint. Under review.

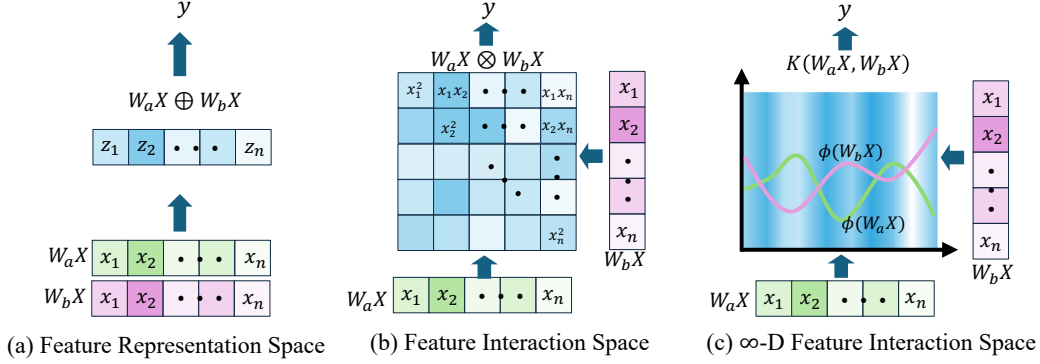


Figure 1: (a) Traditional feature representation without interaction [12, 37]. (b) Recent work with finite feature interaction [31, 41]. (c) Our method: Kernel-enabled infinite feature interaction.

theoretical perspective to rethink the feature interaction scaling, i.e., *the dimensionality of feature interaction space*. For example, as shown in Fig 1(b), by employing the  $\otimes$  multiplication, an implicit interactive quadratic space  $\mathcal{Q} = \text{span}(x_1^2, x_1 x_2, \dots, x_{n-1} x_n, x_n^2)$  with degrees of freedom  $n(n+1)/2$  is constructed from the original representative vector space  $\mathcal{V} = \text{span}(x_1, x_2, \dots, x_n)$  with degrees of freedom  $n$  [26]. Such space dimensionality scaling is the key to improving feature representation quality and end-task, as we will show later.

From the unified perspective, a new opportunity emerges in neural architecture design, that is to scale to *infinite-dimensional feature interactions* than former methodologies (e.g., from  $n(n+1)/2$  to  $\lim_{k \rightarrow \infty} \frac{(n+k-1)!}{(n-1)!k!}$ ). However, scaling feature interaction space dimensionality from architectural enhancements (e.g., quadratic, self-attention, and recursive gates) comes with linear scaling cost w.r.t. order  $k$ , which hinders the infinite dimensionality increase [10, 19]. Thus, there is an open question:

*How can we efficiently extend interactions to an infinite-dimensional space?*

Inspired by traditional machine learning, we propose an approach that introduces kernel methods for feature interaction in neural networks. We define a set of feature interactions between features  $W_a \mathbf{x}$  and  $W_b \mathbf{x}$  with a kernel function  $K(W_a \mathbf{x}, W_b \mathbf{x})$  instead of the element-wise multiplication. As shown in Fig 1(c), the kernel method transforms the feature to an ultra-high dimensional space by an implicit mapping  $\phi(\cdot)$ . From there, the feature interaction space is defined by the inner product on the Reproducing Kernel Hilbert Space (RKHS) [1]  $\mathcal{H}$  constituent with the kernel function  $K(\cdot, \cdot)$ . The RKHS can greatly expand the interaction space at very little cost, enabling infinite dimensions.

We then propose InfiNet, a novel family of neural networks that generate high-quality feature representations. Specifically, we introduce the Radial Basis Function (RBF) kernel [29] as a replacement of the common  $\oplus$  or  $\otimes$  operations. With the infinite series expansion in RBF kernel, it enables a theoretical provable dimensionality approximation  $\text{span}_{j \in \mathbb{N}, \sum_k n_k = j} \left\{ \frac{x_1^{n_1} \dots x_k^{n_k}}{\sqrt{n_1! \dots n_k!}} \right\}$  while with as low-overhead as exponential operations. In this way, InfiNet enables efficient infinite-dimensional feature interaction space scaling upon a finite set of branches in the model architecture, thus achieving better complexity performance tradeoffs than prior state-of-the-arts.

**Contributions.** We make the following contributions:

- We unify the perspectives of recent feature interactive works and identify a novel direction of neural network performance scaling: the feature interaction space dimensionality.
- We propose a method to expand the feature interaction space to an infinite dimension with RBF kernel, that can effectively model the complex implicit correlations of features.
- We propose InfiNet, a novel series of neural networks that explore the neural interaction from infinite-dimensional space, and achieve state-of-the-art performance.

Extensive ablation studies verify that the shift from finite feature interaction space to infinite one is a key factor to learn better representations and therefore improving model performance. Meanwhile, large-scale experiments on ImageNet classification, MS COCO detection and ADE20K segmentation also demonstrate InfiNet design’s effectiveness, which consistently outperforms the state-of-the-art flat stream networks [12, 23] and finite-order interaction networks [22, 31].

## 2 Related Work

**Interactions in Neural Networks.** Interaction in neural networks has undergone a long period of change. During the evolution from AlexNet [16] to ResNet [12], the model has for long followed the principle of summing the weighted pixels at each position in the layer-by-layer feature iteration. And then, as the potential of the attention mechanism was realized, model development is towards an element-wise multiplication way. This trend is punctuated by the emergence of models such as Non-Local [35], Transformer [34], and ViT [10]. Recent insights suggest that the crux of the attention mechanism lies in high-order information interactions, rather than the mechanism of "Attention" itself [3, 31, 39]. This revelation has spurred the development of innovative neural network architectures. For example, HorNet [31], QuadraNet [40] and MogaNet [19] examines high-order models from the perspective of spatial interactions through multiplication-integrated architecture design. However, limited by the support of existing deep learning platforms such as Pytorch [30], few attempts have been made to extend the model's feature interaction to an ultra-high dimensional situation through the kernel method for more potential.

**Kernel Method in Neural Networks.** The fundamentals of kernel methods are well-studied in traditional ML domains like support vector machines [32] but they are less used in neural architectures. Early extensions to deep learning through the kernelized perceptron [6] have improved the performance but mainly in shallow neural networks. Recent advancements include the development of Convolutional Kernel Networks (CKN) [27], which merge CNNs' robust feature learning with kernel stability. This approach offers a theoretical foundation for deep learning's application in structured data. Additionally, the introduction of Kervolutional Neural Networks [5] replaces traditional convolution in CNNs with kernel-based operations to enhance feature extraction without excessive computational costs. The combination of Gaussian processes with neural networks to create Deep Kernel Learning [36] adjusts model complexity based on data while maintaining Bayesian inference.

Despite these innovations, a significant limitation remains: Although these methods expand the feature representation space, they fail to scale up the feature interaction space, limiting the network to aggregate information in a superposition manner. As a result, these methods also fall short of potential feature interactions and thus are incapable of handling complex data correlations and functionalities.

## 3 From Feature Representation Space to Interaction Space

We start with considering the transformation of feature representation of a normal isotropic 2-layer perceptron block. Given an input  $\mathbf{x} = (x_1, x_2, \dots, x_n)$  with  $n$ -dimension. We denote the first layer transformation as  $\mathbf{z} = g(\mathbf{x}) = \sigma(W_1\mathbf{x})$  (we omit the bias term for simplicity), and the second layer transformation as  $h(\mathbf{z}) = W_2\mathbf{z}$ . Therefore the whole block is a mapping  $h \circ g : \mathbb{R}^n \mapsto \mathbb{R}^n \mapsto \mathbb{R}^n$  from feature space  $\mathbb{R}^n$  to a medium feature representation space  $\mathbb{R}^n$  and eventually to a output space  $\mathbb{R}^n$ . Expanding the width of the neural networks, for example with a coefficient 2, is going to expand the feature representation space to  $\mathbb{R}^{2n}$ . The core idea of this dimensional expansion is that implicit associations in feature in low dimensions will be expressed explicitly when projected into a high-dimensional space. Model architecture (i.e. convolution, multi-branch [33]) is an additive superposition of pixels, essentially no different from the perceptron in terms of representation space.

### 3.1 Feature Interaction Space

Although flat stream neural networks are defined by linear transformations and activations, modern network design also introduces multiplications in the network structure or neurons. They are called attentions from an interpretable point of view, that is the degree of interest of one position in relation to another; from a more abstract point of view, they are called interactions in spatial contexts. But invariably, these are realized with element-wise multiplication. We conduct the following definition.

**Definition 1** (Feature Interaction) A Feature interaction refers to transformations between features with the same or different positions defined by element-wise multiplication.

For example, Star Operation [26] is a basic 2-order feature interaction, defined as  $(W_a\mathbf{x}) * (W_b\mathbf{x})$ , where  $W_a, W_b \in \mathbb{R}^n$ . This is a simple element-wise multiplication fusion of two linear transforma-

tions of the ordinary input  $\mathbf{x}$ . We write the expansion of such multiplication operation:

$$y = (W_a \mathbf{x}) * (W_b \mathbf{x}) = \left( \sum_{i=1}^n w_{ai} x_i \right) \left( \sum_{j=1}^n w_{bj} x_j \right) = \sum_{i \leq j} \alpha_{i,j} x_i x_j \quad (1)$$

where  $\alpha_{i,j} = w_{ai}w_{bj} + w_{aj}w_{bi}$ , if  $i \neq j$ , and  $\alpha_{i,i} = w_{ai}w_{bi}$ . Then we vectorize  $\alpha$  and  $x_i x_j$ :

$$A = [\alpha_{1,1}, \alpha_{1,2}, \alpha_{2,2}, \dots, \alpha_{n-1,n}, \alpha_{n,n}] \in \mathbb{R}^{n(n+1)/2} \quad (2)$$

$$\chi = [x_1 x_1, x_1 x_2, x_2 x_2, \dots, x_{n-1} x_n, x_n x_n] \quad (3)$$

$\chi$  can therefore define a basis of a space. Thus the output of the current layer can be rewritten as:

$$y = \sum_{i \leq j} \alpha_{i,j} x_i x_j = A\chi. \quad (4)$$

From the independence of the pixel level, we know that each term in  $\chi$  is linearly independent, this indicates every dimension in  $\chi$  is an individual dimension. Given a set of basis vectors  $\chi$ , we define  $\text{span}(\chi)$  as the feature interaction space. In this way, the generation of the next layer of features  $y$  is constituted by a linear superposition  $A\chi$  on the feature interaction space  $\text{span}(\chi)$  like in Eq.(4).

### 3.2 Dimension of Feature Interaction Space

Now, we consider the number of dimensions of a feature interaction space. Given  $k$ -1 multiplication operations, we first define the  $k$ -order feature interaction space as follows:

**Definition 2** (Feature Interaction Space) A  $k$ -order Feature Interaction Space  $\mathcal{S}^k$  refers to the span of monomial basis  $\{x_1^{d_1} x_2^{d_2} \dots x_n^{d_n} \mid \sum d_i = k, d_i \in \mathbb{N}\}$  defined by a  $k$ -order Feature Interaction.

An element-wise multiplication generates a feature interaction space of  $n(n+1)/2$  dimension, which is the number of elements of an upper triangular matrix. In general, considering the symmetry of the interactions and elements, for a  $k$ -order interaction on the  $n$ -dimensional feature, the dimension of the corresponding feature interaction space is:

$$\dim(\mathcal{S}^k) = \frac{(n+k-1)!}{(n-1)!k!} \quad (5)$$

The next layer of feature generation based on the feature interaction space greatly expands the spatial dimensions to which the features are mapped compared to the original model based only on the feature representation space, i.e., it is possible to explore the feature's non-linearity in high-dimensional space. It is worth noting that this process introduces terms like  $x_1 x_2$ , an interaction that cannot be captured by traditional plane networks in feature representation space.

For example, we consider the Self-Attention in the Transformers [34]. The Self-Attention contains two element-wise multiplication, so it explores a 3-order feature interaction space. This is due to the fact that: (1) in first stage, in the query-key dot-product attention map computation  $\text{Att}(\mathbf{x}) = Q \cdot K^T = W_Q \mathbf{x} \cdot \mathbf{x}^T W_K^T$  explores the feature interaction space  $\mathcal{A} = \text{span}(x_1^2, x_1 x_2, \dots, x_{n-1} x_n, x_n^2)$ . (2) In the second stage, the multiplication between the attention map and the value  $y = \sigma(\text{Att}(\mathbf{x})) \cdot V = \sigma(\text{Att}(\mathbf{x})) \cdot W_v \mathbf{x}$  explores the feature interaction space  $\mathcal{S} = \mathcal{A} \otimes \mathbb{R}^n = \text{span}(x_1^3, x_1^2 x_2, x_1 x_2 x_3, \dots, x_{n-1} x_n^2, x_n^3)$ , which has  $(n+2)(n+1)n/6$  dimensions in line with Eq.(5). Thereby we explain, from the perspective of feature interaction space, why the transformer family of models has, so far, generally outperformed recurrent neural networks and convolutional neural networks in various domains.

## 4 Expanding Interaction Space to Infinite Dimension

This element-wise multiplication-based interaction, since the construction of each order of the feature interaction space is based on a multiplication operator, leads to a problem in that feature interaction space expansion is still difficult. This is due to the fact that these interaction operators is explicit mapping, which tends to have quadratic or higher complexity w.r.t the input length (e.g. self-attention [34]) or lengthy recursive designs (e.g. HorNet [31]) and linear complexity w.r.t interaction order. But the problem with building this mapping explicitly is: (1) The complexity of mapping

itself. The computational overhead associated with defining a set of explicit nonlinear mappings is non-negligible. A mapping from  $C$  channels to  $C'$  channels means a computation complexity of  $O(CC')$ . (2) The complexity of interaction. The complexity of the inner product used to interact with the two sets of features increases dramatically to  $O(C')$  when the dimension is raised. Considering  $C' \gg C$ , these two complexities will largely increase the computational overhead of the networks.

We would like to obtain a method that can expand the dimension of feature interaction space as much as possible in  $O(1)$  time. Fortunately, the machine learning community has already given a method for increasing the dimension of a feature defined on the inner product: **kernel methods**.

#### 4.1 Expanding Interaction Space with Reproducing Kernel

The nature of kernel methods is that they are substitutions for inner product operations. This requires combining element-wise multiplication and summation to define a set of inner products within the network. For this purpose, we rewrite the form of element-wise multiplication in Eq.(1) on two groups of features, which is a common design in literature architecture (e.g. multi-head self-attention [34]). It will therefore be a superposition of multiple interaction in the format:

$$y = \sum_{i=1}^C W_{ai}\mathbf{x} * W_{bi}\mathbf{x} = \langle \mathbf{W}_a\mathbf{x}, \mathbf{W}_b\mathbf{x} \rangle \quad (6)$$

where  $\mathbf{W}_a\mathbf{x} = [W_{a1}\mathbf{x}, W_{a2}\mathbf{x}, \dots, W_{aC}\mathbf{x}]$ ,  $C \in \mathbb{N}$  is the number of branches. Thereby we generalize the form of the feature interaction from element-wise multiplication to inner product which is a multi-branch paradigm. At this point, we have  $\mathbf{W}_a\mathbf{x} \in \mathbb{R}^C$ , while it is generated from a feature representation space  $\mathbb{R}^n$ . In order to extend the interaction space, we need to further project  $\mathbf{W}_a\mathbf{x}$  and  $\mathbf{W}_b\mathbf{x}$  to a high-dimensional space. An obvious way to do this is to construct an implicit mapping  $\Phi(\cdot)$  to a high-dimensional space, so we can compute  $\langle \Phi(W_a\mathbf{x}), \Phi(W_b\mathbf{x}) \rangle$  for interaction.

By Mercer's Theorem [28], taking a continuous symmetric positive semi-definite function  $K(s, t)$ , there is an orthonormal basis  $\{\phi_i(\cdot)\}$ ,  $i = 0, 1, \dots, \infty$ , consisting of eigenfunctions of function  $K(\cdot, \cdot)$  such that the corresponding sequence of eigenvalues  $\{\lambda_i\}$  is non-negative. These means:

$$K(s, t) = \sum_{i=1}^{\infty} \lambda_i \phi_i(s) \phi_i(t), \quad (7)$$

where  $\forall i \neq j, \forall s$  and  $t, \langle \phi_i(s), \phi_j(t) \rangle = 0$  since. Then we construct a Hilbert space  $\mathcal{H}$  with the orthonormal basis  $\{\sqrt{\lambda_i} \phi_i(\cdot)\}$ . Consider a vector  $f = (f_1, f_2, \dots)^T_{\mathcal{H}}$  on the space  $\mathcal{H}$ , then we have:

$$f = \sum_{i=1}^{\infty} f_i \lambda_i \phi_i(\cdot). \quad (8)$$

Thus for a vector  $K(s, \cdot)$  in space  $\mathcal{H}$ :

$$K(s, \cdot) = \sum_{i=1}^{\infty} \lambda_i \phi_i(s) \phi_i(\cdot) = \sum_{i=1}^{\infty} \sqrt{\lambda_i} \phi_i(s) \sqrt{\lambda_i} \phi_i(\cdot) = (\sqrt{\lambda_1} \phi_1(s), \sqrt{\lambda_2} \phi_2(s), \dots)^T_{\mathcal{H}}. \quad (9)$$

Therefore, for the Hilbert space  $\mathcal{H}$ , we can define the reproducing kernel by:

$$\langle K(s, \cdot), K(t, \cdot) \rangle = \sum_{i=1}^{\infty} \sqrt{\lambda_i} \phi_i(s) \sqrt{\lambda_i} \phi_i(t) = \sum_{i=1}^{\infty} \lambda_i \phi_i(s) \phi_i(t). \quad (10)$$

**Implicit Mapping to High-Dimensional RKHS.** Let  $\Phi(s) = K(s, \cdot)$ , then we have  $\langle \Phi(s), \Phi(t) \rangle = K(s, t)$ . The Hilbert Space  $\mathcal{H}$  is known as the Reproducing Kernel Hilbert Space (RKHS) corresponding to kernel function  $K(\cdot, \cdot)$ . Note that the  $\Phi(\cdot)$  is therefore defined on the RKHS  $\mathcal{H}$ , which can be infinite-dimensional given specific kernel  $K(\cdot, \cdot)$ . The mapping  $\Phi(\cdot)$  does not have to have an explicit expression since we can get the result of  $\langle \Phi(s), \Phi(t) \rangle$  by computing  $K(s, t)$ . This means that we can achieve an extension of the dimensions for the feature interaction space by simply replacing the inner product  $\langle \mathbf{W}_a\mathbf{x}, \mathbf{W}_b\mathbf{x} \rangle$  used in the interaction with a kernel  $K(\mathbf{W}_a\mathbf{x}, \mathbf{W}_b\mathbf{x})$ .

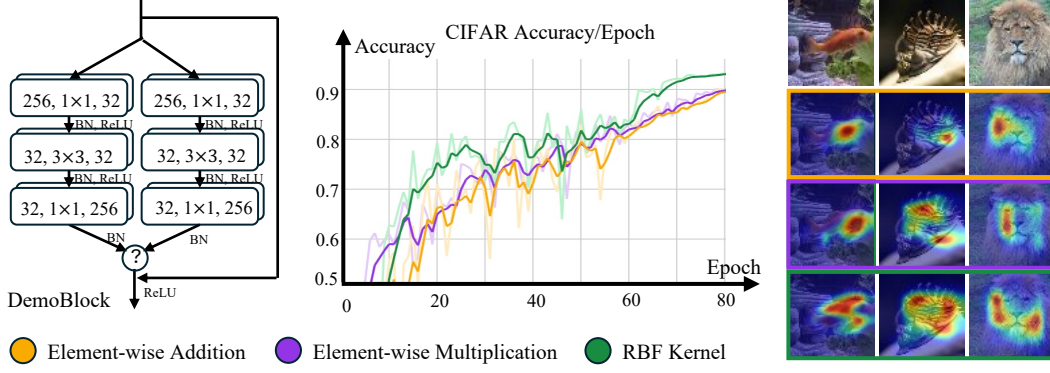


Figure 2: Comparison of simple representation, finite interaction, and infinite-dimensional interaction. The ? circle in DemoBlock is chosen from element-wise Add, element-wise Mul. or RBF kernel.

#### 4.2 Infinite-Dimensional Feature Interaction with RBF Kernel

To maximize the dimension of the feature interaction space, we consider Radial Basis Function (RBF) Kernel  $K_{\text{rbf}}(\mathbf{s}, \mathbf{t}) = \exp\left(-\frac{1}{2}\|\mathbf{s} - \mathbf{t}\|_2^2\right)$  with an infinite-dimensional RKHS, given the fact that:

$$\exp\left(-\frac{1}{2}\|\mathbf{s} - \mathbf{t}\|_2^2\right) = \sum_{j=0}^{\infty} \frac{(\mathbf{s}^\top \mathbf{t})^j}{j!} \exp\left(-\frac{1}{2}\|\mathbf{s}\|_2^2 + \|\mathbf{t}\|_2^2\right) \quad (11)$$

$$= \sum_{j=0}^{\infty} \sum_{n_1+n_2+\dots+n_k=j} \exp\left(-\frac{1}{2}\|\mathbf{s}\|_2^2\right) \frac{s_1^{n_1} \dots s_k^{n_k}}{\sqrt{n_1! \dots n_k!}} \exp\left(-\frac{1}{2}\|\mathbf{t}\|_2^2\right) \frac{t_1^{n_1} \dots t_k^{n_k}}{\sqrt{n_1! \dots n_k!}} \quad (12)$$

$$= \langle \Phi_{\text{rbf}}(\mathbf{s}), \Phi_{\text{rbf}}(\mathbf{t}) \rangle, \quad (13)$$

where  $\Phi_{\text{rbf}}(\mathbf{x}) = \sum_{j=0}^{\infty} \sum_{\sum_k n_k=j} \exp\left(-\frac{1}{2}\|\mathbf{x}\|_2^2\right) \frac{s_1^{n_1} \dots s_k^{n_k}}{\sqrt{n_1! \dots n_k!}} \in \text{span}_{j \in \mathbb{N}, \sum_k n_k=j} \left\{ \frac{x_1^{n_1} \dots x_k^{n_k}}{\sqrt{n_1! \dots n_k!}} \right\}$ .

**Infinite-dimensional Feature Interaction Space** Observing the RKHS of such a RBF kernel,  $\text{span}_{j \in \mathbb{N}, \sum_k n_k=j} \left\{ \frac{x_1^{n_1} \dots x_k^{n_k}}{\sqrt{n_1! \dots n_k!}} \right\}$ , We note that each of its dimensions is a  $j$ -order interaction within the feature  $\mathbf{x}$ , given the fact one of the bases of this RKHS is:

$$\{1, x_1, \dots, x_n, x_1^2, \dots, x_1 x_n, \dots, x_n^2, \dots, x_1^j, x_1^{j-1} x_2, \dots, x_n^j, \dots\}, \quad (14)$$

which contains an all-order monomial among all elements of the feature  $\mathbf{x}$ . This means that we get an infinite-dimensional Hilbert space for the superposition of interaction information through such an RBF kernel, and most importantly, each dimension of this space is defined by a feature interaction. Therefore, we get an infinite-dimensional feature interaction space.

#### 4.3 Demo Case Performance of Models on Different Feature Space

In order to compare networks that utilize the summing superposition of information mappings on the feature representation space, finite feature interaction space, and infinite-dimensional interaction space, we design a demo network with 8 DemoBlock, as shown in Fig. 2. DemoBlock has a two-group design, the only difference among models in different spaces is the interaction method at the end of the block (add for simple representation, multiplication for finite interaction, and RBF kernel for infinite dimensional interaction), the demo models are trained on CIFAR10 and Tiny-ImageNet.

As shown in Fig. 2, with the procedure of transferring from the simple feature representation space to a finite feature interaction and eventually to an infinite-dimensional interaction, the performance on CIFAR10 of the networks is growing. This is done throughout the training process, implying the superiority of feature iteration in a high-dimensional interaction space. The right side of Fig. 2 shows the Class Activation Mapping [43] of three different demo nets on Tiny-ImageNet. From this, we can see that the network of feature interaction better reflects the pixel-level correlation within the image.

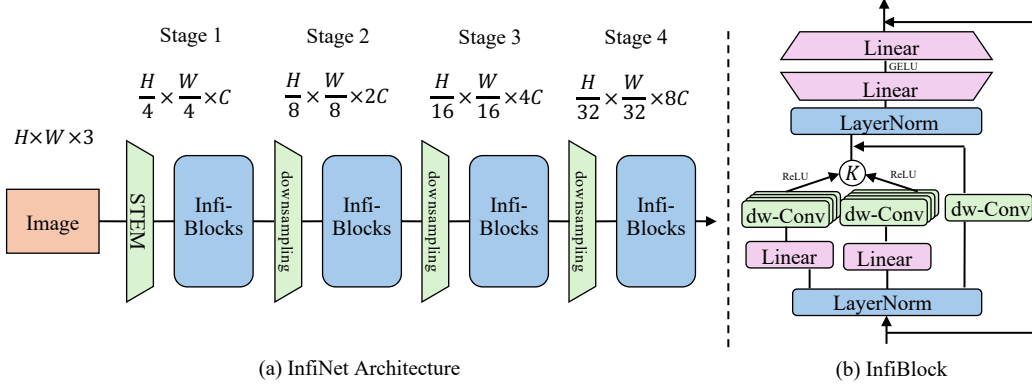


Figure 3: **Overview of InfiNet.** (a) Four-stage hierarchical InfiNet design. (b) InfiBlock Design

## 5 Method

### 5.1 InfiBlock: Infinite-Dimensional Spatial Feature Interaction

**InfiBlock.** In this section, we present InfiBlock, the basic block to build the high-performant InfiNet architecture to achieve infinite-dimensional spatial feature interaction. As presented in Fig. 3(b), InfiBlock starts with a LayerNorm layer and subsequently transforms the feature into separate representations of the two groups through two different linear layers. Then InfiBlock utilizes a depth-width convolution with an expansion coefficient of  $r$  and a ReLU activation to obtain a feature branch vector of length  $r$  on each group. The feature branch vectors on both groups are then fed into an RBF kernel for feature interaction. At the same time, we retain a pathway containing only one depth-wise convolution for summing superposition over the feature representation space to ensure that the linear connections between features are not neglected and overfitted. This is followed by a residual connection with the original input values after passing through a two-layer MLP. Starting with an input  $X^l \in \mathbb{R}^{HWC}$ , Infi-Block can be formulated as:

$$\hat{X}^l = \text{LayerNorm}(X^l), \quad (15)$$

$$[\bar{Z}_a^l, \bar{Z}_b^l, Z_c^l] = [\sigma(\text{Conv}_a(\hat{X}^l W_a)), \sigma(\text{Conv}_b(\hat{X}^l W_b)), \text{Conv}_c(\hat{X}^l)], \quad (16)$$

$$X^{l+1} = \text{MLP}(\text{LayerNorm}(K_{rbf}(\bar{Z}_a^l, \bar{Z}_b^l) + Z_c^l)) + X^l, \quad (17)$$

where  $K_{rbf}(\bar{Z}_a^l, \bar{Z}_b^l) = \exp(-\frac{\|\bar{Z}_a^l - \bar{Z}_b^l\|_2^2}{2})$ , is an RBF kernel with out any hyper-parameter, and  $\|\cdot\|_2^2$  is squared L-2 norm.  $\text{LayerNorm}(\cdot)$  is layer normalization [2] and  $\text{MLP}(\cdot)$  is activated by GELU [13].

Specifically, following the ConvNeXt [23], we select a  $7 \times 7$  depth-wise convolution to obtain a larger receptive field. We set the expansion coefficient  $r$  as 7 in practice. This means:

$$[\bar{Z}_a^l, \bar{Z}_b^l] = [[Z_{a1}^l, Z_{a2}^l, \dots, Z_{a7}^l]^T, [Z_{b1}^l, Z_{b2}^l, \dots, Z_{b7}^l]^T], \quad (18)$$

where  $Z_{ai}^l = \sigma(\text{DW-Conv}_{ai}(X^l W_a)) \in \mathbb{R}^{HWC}$ . Therefore, the RBF kernel performs feature interaction on multiple (7) branches of convolution filter and outputs a result still in  $\mathbb{R}^{HWC}$ .

### 5.2 Model Architectures

As shown in Fig. 3(a), InfiNet uses the widely adopted 4-stage hierarchical architecture as in ResNet [12], ConvNeXt [23] and Swin Transformer [22]. We stack InfiBlocks into each stage. We set the number of channels in each stage as  $[C, 2C, 4C, 8C]$  following common practice. We build a family of InfiNets that InfiNet-T/S/B/L/XL with model variants hyper-parameters:  $C = \{64, 96, 128, 128, 192\}$ , number of blocks in each stages =  $\{2, 2, 18, 2\}$  for InfiNet-T/S/B and  $\{3, 3, 27, 3\}$  for InfiNet-L/XL. A down-sampling with  $2 \times 2$  convolution with stride = 2 is used to connect each stage. STEM [23] is used to connect the input of InfiNet to Stage 1.

Table 1: **ImageNet classification results.** We compare our models with state-of-the-art models with comparable parameters, the Top-1 accuracy is reported on the ImageNet-1K validation set.

Model	Interact. Orders	Params (M)	FLOPs (G)	Top1 Acc.(%)	Model	Interact. Orders	Params (M)	FLOPs (G)	Top1 Acc.(%)
ConvNeXt-T[23]	no	29	4.5	82.1	ConvNeXt-B[23]	no	89	15.4	83.8
SLaK-T[21]	no	30	5.0	82.5	SLaK-B[21]	no	85	17.1	84.0
Conv2Former-T[14]	2	27	4.4	83.1	Conv2Former-B[14]	2	90	15.9	84.4
UniFormer-S[18]	2	22	3.6	82.9	CoAtNet-2[7]	3	75	15.7	84.1
CoAtNet-0[7]	3	25	4.2	82.7	FocalNet-B[42]	3	89	15.4	83.9
FocalNet-T[42]	3	28	4.4	82.1	Swin-B[22]	3	89	15.4	83.5
Swin-T[22]	3	28	4.5	81.3	HorNet-B[31]	2-5	87	15.6	84.3
HorNet-T[31]	2-5	22	4	82.8	MogaNet-L[19]	4	83	15.9	83.5
MogaNet-S[19]	4	25	5.0	83.5	<b>InfiNet-B</b>	$\infty$	82	12.8	84.5
<b>InfiNet-T</b>	$\infty$	23	3.2	83.4	<b>InfiNet-L</b>	$\infty$	116.8	19.1	84.8
<i>ImageNet-21K Pretrained Models Fine-tuned @384<sup>2</sup></i>									
ConvNeXt-S[23]	no	50	8.7	83.1	ConvNeXt-L <sup>‡</sup> [23]	no	198	101	87.5
SLaK-S[21]	no	55	9.8	83.8	CoAtNet-3 <sup>‡</sup> [7]	3	168	107	87.6
Conv2Former-S[14]	2	50	8.7	84.1	FocalNet-L <sup>‡</sup> [42]	3	197	101	87.3
UniFormer-B[18]	2	50	8.3	83.9	Swin-L <sup>‡</sup> [22]	3	197	104	87.3
CoAtNet-1[7]	3	42	8.4	83.3	HorNet-L <sup>‡</sup> [31]	2-5	202	102	87.7
FocalNet-S[42]	3	50	8.7	83.5	MogaNet-XL <sup>‡</sup> [19]	4	181	102	87.8
Swin-S[22]	3	50	8.7	83.0	<b>InfiNet-L<sup>‡</sup></b>	$\infty$	116.8	60	87.8
HorNet-S[31]	2-5	50	8.8	84.0	ConvNeXt-XL <sup>‡</sup> [23]	no	350	179	87.8
MogaNet-B[19]	4	44	9.9	84.3	<b>InfiNet-XL<sup>‡</sup></b>	$\infty$	255.8	126	88.2

## 6 Experiments

We perform a series of experiments to validate the efficacy of InfiNets. The primary results on ImageNet [8] are showcased and contrasted with several architectures. Furthermore, our models were evaluated on downstream ADE20K[44] semantic segmentation and COCO [20] object detection. ImageNet-1K experiments are conducted on 4×Nvidia A100 GPUs and ImageNet-21K on 16×.

### 6.1 ImageNet Classification

**Setups.** We conduct image classification experiments on ImageNet-1K [8], which contains 1.28 million training samples belonging to 1000 classes and 50K samples for validation. We train the InfiNet-T/S/B/L models for 300 epochs with AdamW [25] optimizer. We use the cosine learning rate scheduler [24] with 20 warmup epochs and the basic learning rate is set as  $4 \times 10^{-3}$ . The training resolution is set as  $224 \times 224$ . To further evaluate the InfiNet’s scalability, we train the InfiNet-L/XL models on 14M-sample ImageNet-22K dataset for 90 epochs and then fine-tune on ImageNet-1K at  $384 \times 384$  resolution for 30 epochs following [23]. More details can be found in Appendix A.1.

**Results.** We present our ImageNet experiment results and comparison with baselines in Table 1. Our models achieve competitive performance with state-of-the-art. It is worth noting that InfiNet has about 20% fewer FLOPs than the baseline models with similar parameter scales, but still achieves great performance. It demonstrates the effectiveness of our proposed generation of features in infinite-dimensional interaction spaces. Experiments on isotropic models can be found in Table 3(a).

### 6.2 MS COCO Detection

**Setups.** We evaluate our models for object detection tasks on widely used MS COCO [20] benchmark. In the experiments, InfiNet-T/S/b/XL serves as the backbone network within Cascade Mask RCNN [4]. We use AdamW as the optimizer and a batch size of 16 and adhere to the  $3 \times$  schedule, following ConvNeXt [23] and Swin [22]. We resize the input so that the longer side is at most 1333 and the short side is at most 800. We initialize the backbone model with ImageNet-1K pre-trained weights for T/S/B models and ImageNet-22K pre-trained weights for XL model.

**Results.** As shown in Table 2, InfiNets comprehensively beat the non-interactive model ConvNeXt [23], and space-limited interactive Swin [22] and HorNet [31] under the same cascade Mask RCNN framework in box AP and mask AP. This means that for such dense prediction tasks, spatial interaction of features in a high-dimension space is crucial. The InfiNet series model obtain 0.9 ~ 1.5 box AP and 1.3 ~ 2.5 mask AP gain compared with non-interactive ConNeXt.



Table 2: Object detection and semantic segmentation results on MS COCO and ADE20K.

Model	Object Detection with <i>Cascade Mask R-CNN 3×</i>				Semantic Segmentation with <i>UperNet 160K</i>			
	AP <sup>box</sup>	AP <sup>mask</sup>	Params	FLOPs	mIoU <sup>ss</sup>	mIoU <sup>ms</sup>	Params	FLOPs
ConvNeXt-T[23]	50.4	43.7	86M	741G	46.0	46.7	60M	939G
Swin-T[22]	50.4	43.7	86M	745G	44.5	45.8	60M	945G
HorNet-T[31]	51.7	44.8	80M	730G	48.1	48.9	52M	926G
<b>InfiNet-T</b>	51.9	46.2	77M	724G	46.7	47.4	50M	924G
ConvNeXt-S[23]	51.9	45.0	108M	827G	48.7	49.6	82M	1027G
Swin-S[22]	51.8	44.7	107M	838G	47.6	49.5	81M	1038G
HorNet-S[31]	52.7	45.6	107M	830G	49.2	49.8	81M	1030G
<b>InfiNet-S</b>	52.8	46.4	98M	802G	49.4	49.9	78M	1002G
ConvNeXt-B[23]	52.7	45.6	146M	964G	49.1	49.9	122M	1170G
Swin-B[22]	51.9	45.0	145M	982G	48.1	49.7	121M	1188G
HorNet-B[31]	53.3	46.1	144M	969G	50.0	50.5	121M	1174G
<b>InfiNet-B</b>	53.7	47.3	126M	906G	50.2	50.9	105M	1111G
ConvNeXt-L <sup>†</sup> [23]	54.8	47.6	255M	1354G	53.2	53.7	235M	2458G
Swin-L <sup>†</sup> [22]	53.9	46.7	253M	1382G	52.1	53.5	234M	2468G
HorNet-L <sup>†</sup> [31]	55.4	48.0	251M	1363G	54.1	54.5	232M	2473G
<b>InfiNet-XL<sup>†</sup></b>	56.3	48.9	273M	1454G	54.6	55.2	253M	2544G

Table 3: More Results on isotropic models and different kind of Reproducing Kernel

(a) Isotropic Models					(b) Ablation Study				
Model	Interact. Orders	Params (M)	FLOPs (G)	Top1 Acc.(%)	Model	Interact. Orders	Params (M)	FLOPs (G)	Top1 Acc.(%)
ConvNeXt-S(iso.)	no	22	4.3	79.7	InfiNet- $\oplus$	no	23	3.2	81.6
Conv2Former(iso.)	2	23	4.3	81.2	InfiNet- $\otimes$	2	23	3.2	82.1
DeiT-S[23]	3	22	4.6	79.8	InfiNet-2-polyno.	4	23	3.2	82.3
HorNet-S(iso.)	2-5	22	4.5	80.6	InfiNet-3-polyno.	6	23	3.2	82.5
<b>InfiNet-S(iso.)</b>	$\infty$	22	4.3	81.4	<b>InfiNet-T</b>	$\infty$	23	3.2	83.4

### 6.3 ADE20 Segmentation

**Setups.** We evaluate our models for the semantic segmentation task on widely used ADE20K [44] benchmark covering 150 semantic categories on 25K images, in which 20K are used for training. We use UperNet [38] for as the basic framework and adopt InfiNets as the backbone model. Training details follow the Swin [22], we use AdamW optimizer with learning rate  $1 \times 10^{-4}$  and batch size 16.

**Results.** The right half of Table 2 lists the mIoU and corresponding model size and FLOPs for different configurations. Our models beat most of the baseline in the segmentation task. The results show that as the model size increases, the performance gap between InfiNet and other baselines is getting larger, illustrating the scalability of InfiNet on segmentation.

### 6.4 Ablation Study

We use the additive operator, Hadamard product, quadratic polynomial kernel and cubic polynomial kernel, and RBF kernel in the kernel methods section of InfiNet, respectively, on a tiny size model, to verify the effect of the gradual expansion of the order of the interaction space up to infinite dimensions on the performance of the model. As in Table 3(b), we can see that the performance of the model is gradually improving as the order of the model interaction space increases up to infinite dimensions.

## 7 Conclusion

As a conclusion, in this paper, we propose that one of the key points of success of today’s element-wise multiplication-based models is that they explore a high-dimensional feature interaction space through feature interactions. And the RBF kernel can greatly expand this interaction space into an infinite dimensional feature interaction space. Based on this observation, we propose InfiNet, a high-performance neural network that explores infinite-dimensional feature interactions while using a modern model structure, which has achieved state-of-the-art results on several visual tasks.

## References

- [1] N. Aronszajn. Theory of reproducing kernels. *Transactions of the American mathematical society*, 68(3):337–404, 1950.
- [2] J. L. Ba, J. R. Kiros, and G. E. Hinton. Layer normalization. *arXiv preprint arXiv:1607.06450*, 2016.
- [3] B. Bai, J. Liang, G. Zhang, H. Li, K. Bai, and F. Wang. Why attentions may not be interpretable? In *Proceedings of the 27th ACM SIGKDD conference on knowledge discovery & data mining*, pages 25–34, 2021.
- [4] Z. Cai and N. Vasconcelos. Cascade r-cnn: Delving into high quality object detection. In *Proceedings of the IEEE conference on computer vision and pattern recognition*, pages 6154–6162, 2018.
- [5] C. Chen, M. Seuret, M. Liwicki, J. Hennebert, and R. Ingold. Kervolutional neural networks. *arXiv preprint arXiv:1904.03955*, 2019.
- [6] Y. Cho and L. K. Saul. Kernel methods for deep learning. In *Advances in neural information processing systems*, pages 342–350, 2009.
- [7] Z. Dai, H. Liu, Q. V. Le, and M. Tan. Coatnet: Marrying convolution and attention for all data sizes. *Advances in neural information processing systems*, 34:3965–3977, 2021.
- [8] J. Deng, W. Dong, R. Socher, L.-J. Li, K. Li, and L. Fei-Fei. Imagenet: A large-scale hierarchical image database. In *2009 IEEE conference on computer vision and pattern recognition*, pages 248–255. Ieee, 2009.
- [9] E. Dohmatob, Y. Feng, P. Yang, F. Charton, and J. Kempe. A tale of tails: Model collapse as a change of scaling laws. *International Conference on Machine Learning*, 2024.
- [10] A. Dosovitskiy, L. Beyer, A. Kolesnikov, D. Weissenborn, X. Zhai, T. Unterthiner, M. Dehghani, M. Minderoeder, G. Heigold, S. Gelly, et al. An image is worth 16x16 words: Transformers for image recognition at scale. In *International Conference on Learning Representations*, 2020.
- [11] F.-L. Fan, H.-C. Dong, Z. Wu, L. Ruan, T. Zeng, Y. Cui, and J.-X. Liao. One neuron saved is one neuron earned: On parametric efficiency of quadratic networks. *arXiv preprint arXiv:2303.06316*, 2023.
- [12] K. He, X. Zhang, S. Ren, and J. Sun. Deep residual learning for image recognition. In *Proceedings of the IEEE conference on computer vision and pattern recognition*, pages 770–778, 2016.
- [13] D. Hendrycks and K. Gimpel. Gaussian error linear units (gelu). *arXiv preprint arXiv:1606.08415*, 2016.
- [14] Q. Hou, C.-Z. Lu, M.-M. Cheng, and J. Feng. Conv2former: A simple transformer-style convnet for visual recognition. *IEEE Transactions on Pattern Analysis and Machine Intelligence*, 2024.
- [15] J. Hu, L. Shen, and G. Sun. Squeeze-and-excitation networks. In *Proceedings of the IEEE conference on computer vision and pattern recognition*, pages 7132–7141, 2018.
- [16] A. Krizhevsky, I. Sutskever, and G. E. Hinton. Imagenet classification with deep convolutional neural networks. *Advances in neural information processing systems*, 25, 2012.
- [17] Y. LeCun, L. Bottou, Y. Bengio, and P. Haffner. Gradient-based learning applied to document recognition. *Proceedings of the IEEE*, 86(11):2278–2324, 1998.
- [18] K. Li, Y. Wang, G. Peng, G. Song, Y. Liu, H. Li, and Y. Qiao. Uniformer: Unified transformer for efficient spatial-temporal representation learning. In *International Conference on Learning Representations*, 2022.
- [19] S. Li, Z. Wang, Z. Liu, C. Tan, H. Lin, D. Wu, Z. Chen, J. Zheng, and S. Z. Li. Moganet: Efficient multi-order gated aggregation network. *International Conference on Learning Representation*, 2024.
- [20] T.-Y. Lin, M. Maire, S. Belongie, J. Hays, P. Perona, D. Ramanan, P. Dollár, and C. L. Zitnick. Microsoft coco: Common objects in context. In *Computer Vision—ECCV 2014: 13th European Conference, Zurich, Switzerland, September 6-12, 2014, Proceedings, Part V 13*, pages 740–755. Springer, 2014.
- [21] S. Liu, T. Chen, X. Chen, X. Chen, Q. Xiao, B. Wu, T. Kärkkäinen, M. Pechenizkiy, D. C. Mocanu, and Z. Wang. More convnets in the 2020s: Scaling up kernels beyond 51x51 using sparsity. In *The Eleventh International Conference on Learning Representations*, 2023.
- [22] Z. Liu, Y. Lin, Y. Cao, H. Hu, Y. Wei, Z. Zhang, S. Lin, and B. Guo. Swin transformer: Hierarchical vision transformer using shifted windows. In *Proceedings of the IEEE/CVF international conference on computer vision*, pages 10012–10022, 2021.
- [23] Z. Liu, H. Mao, C.-Y. Wu, C. Feichtenhofer, T. Darrell, and S. Xie. A convnet for the 2020s. In *Proceedings of the IEEE/CVF conference on computer vision and pattern recognition*, pages 11976–11986, 2022.
- [24] I. Loshchilov and F. Hutter. SGDR: Stochastic gradient descent with warm restarts. In *International Conference on Learning Representations*, 2017.
- [25] I. Loshchilov and F. Hutter. Decoupled weight decay regularization. In *International Conference on Learning Representations*, 2019.

- [26] X. Ma, X. Dai, Y. Bai, Y. Wang, and Y. Fu. Rewrite the stars. *Proceedings of the IEEE/CVF conference on computer vision and pattern recognition*, 2024.
- [27] J. Mairal, P. Koniusz, Z. Harchaoui, and C. Schmid. Convolutional kernel networks. In *Advances in neural information processing systems*, pages 2627–2635, 2014.
- [28] J. Mercer. Xvi. functions of positive and negative type, and their connection the theory of integral equations. *Philosophical transactions of the royal society of London. Series A, containing papers of a mathematical or physical character*, 209(441-458):415–446, 1909.
- [29] M. T. Musavi, W. Ahmed, K. H. Chan, K. B. Faris, and D. M. Hummels. On the training of radial basis function classifiers. *Neural networks*, 5(4):595–603, 1992.
- [30] A. Paszke, S. Gross, F. Massa, A. Lerer, J. Bradbury, G. Chanan, T. Killeen, Z. Lin, N. Gimelshein, L. Antiga, et al. Pytorch: An imperative style, high-performance deep learning library. *Advances in neural information processing systems*, 32, 2019.
- [31] Y. Rao, W. Zhao, Y. Tang, J. Zhou, S. N. Lim, and J. Lu. Hornet: Efficient high-order spatial interactions with recursive gated convolutions. *Advances in Neural Information Processing Systems*, 35:10353–10366, 2022.
- [32] B. Schölkopf, A. Smola, and K.-R. Müller. Nonlinear component analysis as a kernel eigenvalue problem. *Neural computation*, 10(5):1299–1319, 1998.
- [33] C. Szegedy, W. Liu, Y. Jia, P. Sermanet, S. Reed, D. Anguelov, D. Erhan, V. Vanhoucke, and A. Rabinovich. Going deeper with convolutions. In *Proceedings of the IEEE conference on computer vision and pattern recognition*, pages 1–9, 2015.
- [34] A. Vaswani, N. Shazeer, N. Parmar, J. Uszkoreit, L. Jones, A. N. Gomez, L. Kaiser, and I. Polosukhin. Attention is all you need. *Advances in neural information processing systems*, 30, 2017.
- [35] X. Wang, R. Girshick, A. Gupta, and K. He. Non-local neural networks. In *Proceedings of the IEEE conference on computer vision and pattern recognition*, pages 7794–7803, 2018.
- [36] A. G. Wilson, Z. Hu, R. Salakhutdinov, and E. P. Xing. Deep kernel learning. In *Artificial intelligence and statistics*, pages 370–378, 2016.
- [37] S. Woo, S. Debnath, R. Hu, X. Chen, Z. Liu, I. S. Kweon, and S. Xie. Convnext v2: Co-designing and scaling convnets with masked autoencoders. In *Proceedings of the IEEE/CVF Conference on Computer Vision and Pattern Recognition*, pages 16133–16142, 2023.
- [38] T. Xiao, Y. Liu, B. Zhou, Y. Jiang, and J. Sun. Unified perceptual parsing for scene understanding. In *Proceedings of the European conference on computer vision (ECCV)*, pages 418–434, 2018.
- [39] C. Xu, X. Wang, F. Yu, J. Xiong, and X. Chen. Quadranet v2: Efficient and sustainable training of high-order neural networks with quadratic adaptation. *arXiv preprint arXiv:2405.03192*, 2024.
- [40] C. Xu, F. Yu, Z. Xu, C. Liu, J. Xiong, and X. Chen. Quadranet: Improving high-order neural interaction efficiency with hardware-aware quadratic neural networks. *The 29th Asia and South Pacific Design Automation Conference*, 2024.
- [41] Z. Xu, F. Yu, J. Xiong, and X. Chen. Quadralib: A performant quadratic neural network library for architecture optimization and design exploration. *Proceedings of Machine Learning and Systems*, 4:503–514, 2022.
- [42] J. Yang, C. Li, X. Dai, and J. Gao. Focal modulation networks. *Advances in Neural Information Processing Systems*, 35:4203–4217, 2022.
- [43] B. Zhou, A. Khosla, A. Lapedriza, A. Oliva, and A. Torralba. Learning deep features for discriminative localization. In *Proceedings of the IEEE conference on computer vision and pattern recognition*, pages 2921–2929, 2016.
- [44] B. Zhou, H. Zhao, X. Puig, S. Fidler, A. Barriuso, and A. Torralba. Scene parsing through ade20k dataset. In *Proceedings of the IEEE conference on computer vision and pattern recognition*, pages 633–641, 2017.

## A Appendix

### A.1 Training Details

The training details for ImageNet experiments are shown in Table 4 and Table 5.

Table 4: Training details for ImageNet-1K experiments

Configuration	InifNet-T/S/B/L
Input resolution	224 <sup>2</sup>
Epochs	300
Batch size	192/128/64/64
Optimizer	AdamW
AdamW ( $\beta_1, \beta_2$ )	0.9, 0.999
Learning rate	0.004
Learning rate decay	Cosine
Weight decay	0.05
Warmup epochs	20
Label smoothing $\epsilon$	0.1
Stochastic Depth	Y
Rand Augment	9/0.5
Repeated Augment	Y
Erasing prob.	0.25
ColorJitter	N
Gradient Clipping	Y
EMA decay	Y

Table 5: Training details for ImageNet-21K experiments

Configuration	IN-21K PT		IN-1K FT	
	L	XL	L	XL
Input resolution	224 <sup>2</sup>		384 <sup>2</sup>	
Epochs	90		30	
Batch size	256		64	
Optimizer	AdamW		AdamW	
AdamW ( $\beta_1, \beta_2$ )	0.9, 0.999		0.9, 0.999	
Learning rate	$4 \times 10^{-3}$		$5 \times 10^{-5}$	
Learning rate decay	Cosine		Cosine	
Weight decay	0.1		0.00001	
Warmup epochs	5		0	
Label smoothing $\epsilon$	0.2		0.1	0.2
Rand Augment	9/0.5		9/0.5	
Repeated Augment	N		N	
Erasing prob.	0.25		0.25	
Gradient Clipping	5		5	
EMA decay	N		Y	

### A.2 More Visualization Comparison

In Fig. 4, we provide more Class Activation Mapping to illustrate the interpretability of interaction models. Infinite-dimensional Interaction models capture more totality of objects within a category, illustrates the importance of this infinite-dimensional interaction.

### A.3 Limitations

Although we explored polynomial kernels and RBF kernels, there are still a wide variety of kernel methods that we did not explore, including a learnable kernel. In addition, to avoid additional

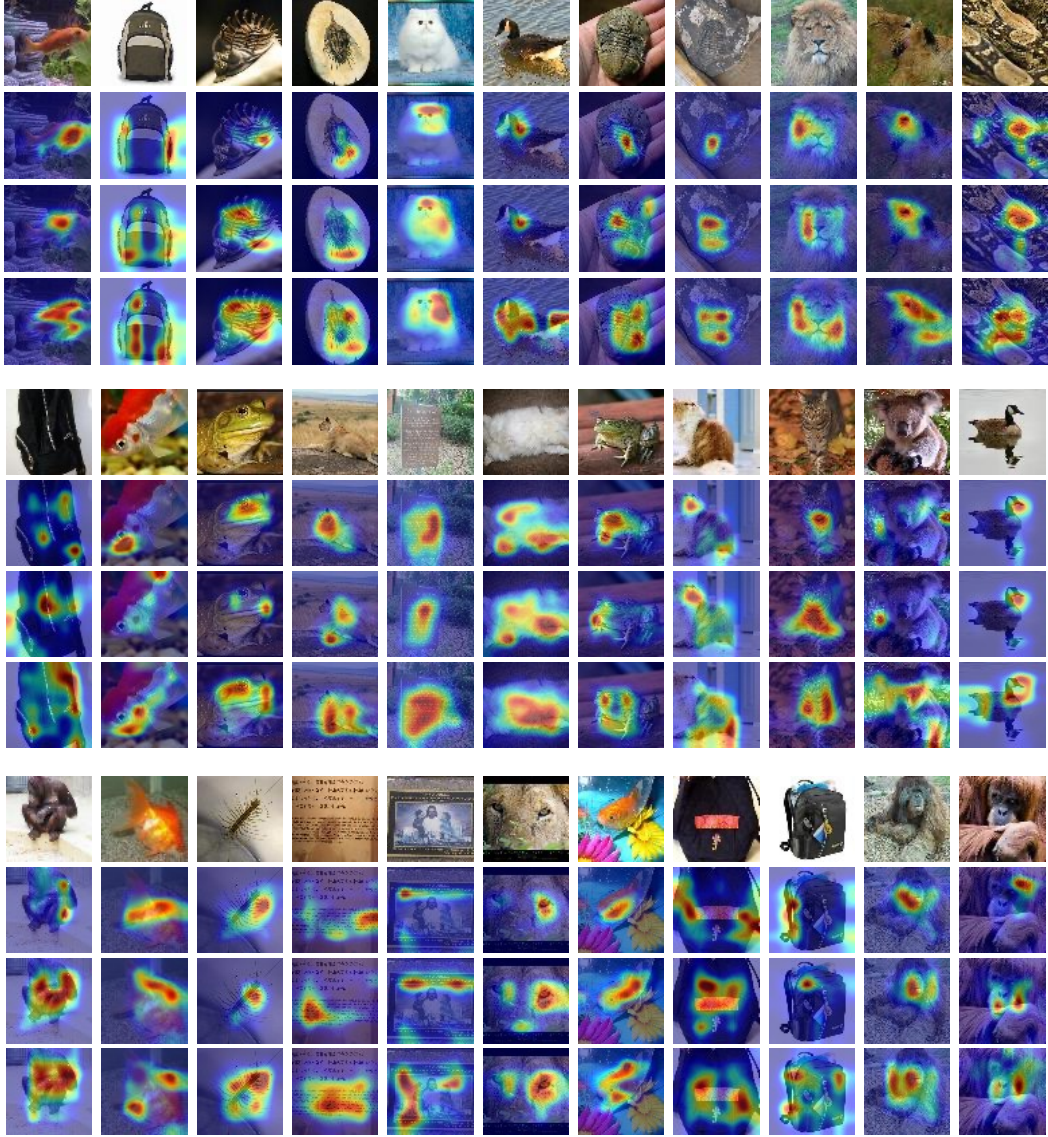


Figure 4: Visualization Comparison of (1) Feature Representation Space model, (2) Finite Feature Interaction Space model, (3) Infinite-Dimensional Feature Interaction model

hyperparameter tuning, we fixed the  $\sigma$  parameter in the RBF kernel to 1. This may have deprived us of the possibility of exploring the optimal InfiNet, but due to the high cost of training the model, we will leave the impact of this hyperparameter on the InfiNet as a follow-up work.

#### A.4 Broader Social Impact

InfiNet is a state-of-the-art vision neural network architecture. The advancements in computer vision neural network architectures hold significant potential for positive societal impact, particularly in enhancing healthcare diagnostics, improving security systems, and advancing autonomous transportation. However, it is crucial to address potential negative implications such as privacy concerns, algorithmic biases, and job displacement. Ensuring ethical development and deployment involves implementing strict data protection measures, promoting fairness and inclusivity in algorithm design, and supporting workforce retraining programs. By proactively managing these challenges, we can maximize the benefits of computer vision technologies while minimizing their risks. Engaging with diverse stakeholders will be essential to ensure these technologies are used responsibly and equitably.